Available online at www.sciencedirect.com
ScienceDirect
Journal of Catalysis 256 (2008) 145–153
JOURNAL OF CATALYSIS
www.elsevier.com/locate/jcat

Is there a relationship between the M=O bond length (strength) of bulk mixed metal oxides and their catalytic activity?

Kamalakanta Routray [a], Laura E. Briand [b], Israel E. Wachs [a,*]

[a] *Operando Molecular Spectroscopy and Catalysis Laboratory, Chemical Engineering Department, 111 Research Drive, Lehigh University, Bethlehem, PA 18015, USA*

[b] *Centro de Investigacion y Desarrollo en Ciencias Aplicadas–Dr. Jorge J. Ronco, Universidad Nacional de La Plata, Calle 47 No. 257 (1900), La Plata, Buenos Aires, Argentina*

Received 1 January 2008; revised 8 March 2008; accepted 10 March 2008

Abstract

It is widely accepted in the catalysis literature that the bulk M=O bond of bulk mixed metal oxides controls catalytic activity. In the present study, for the first time, the bulk M=O bond lengths (strengths) and the surface catalytic activity of bulk metal vanadates and molybdates were quantitatively compared to allow examination of this long-standing hypothesis. The bulk M=O bond lengths were obtained from crystallographic studies and also determined by Raman spectroscopy. The surface catalytic activity was determined by CH_3OH-temperature programmed surface reaction (TPSR) spectroscopy and steady-state methanol oxidation. The CH_3OH-TPSR experiments provided the first-order rate constants for breaking of the C–H bond for the decomposition of the surface CH_3O^* intermediate to H_2CO and the number of catalytic active sites (N_s). The corresponding steady-state methanol oxidation studies provided the equilibrium adsorption constant (K_{ads}) for breaking the methanol O–H bond and the specific reaction rate (TOF). The findings clearly demonstrate the lack of correlations among k_{rds}, K_{ads}, TOF, and the bulk M=O bond length (strength). This finding is not so surprising when one considers that the adsorption step involves breaking the methanol O–H bond and the rate-determining step involves breaking the surface methoxy C–H bond on *surface* MO_x sites, not *bulk* M=O bond-breaking.

Keywords: Catalysts, metal oxides, molybdates, vanadates; Reaction, oxidation, methanol (CH_3OH), formaldehyde (H_2CO); Spectroscopy; Raman; TPSR

1. Introduction

Bulk mixed metal oxides widely used as selective oxidation catalysts for the industrial production of chemical intermediates; major applications include the oxidation of methanol to formaldehyde using bulk iron molybdate [1], the oxidation of propylene to acrolein [2] and the further oxidation of acrolein to acrylic acid using bulk bismuth molybdate [2], the selective ammoxidation of propylene to acrylonitrile with bulk bismuth molybdates [2], and the oxidation of *n*-butane to maleic anhydride over bulk vanadyl pyrophosphate [3]. The significant industrial applications of bulk mixed metal oxide catalytic materials have led to much research aimed at providing insight into their structure–activity relationships.

According to the catalysis literature, the short M=O bond in bulk mixed metal oxides is the catalytic active site responsible for catalytic activity. Mars and van Krevelen were the first to suggest that the short V=O bond was the catalytic active site in oxidation reactions [4]. Trifiro et al. concluded that the oxidative dehydrogenating power of metal oxide catalysts, such as bulk V_2O_5, MoO_3, mixed metal vanadates, and molybdates, is related to the strength of the short M=O bond [5]. This conclusion was reached for bulk mixed metal molybdates based on a qualitative relationship between the IR Mo=O bond strength (lower IR cm^{-1} values, corresponding to weaker Mo=O bond strength) and the catalytic activity for CH_3OH oxidative dehydrogenation. It was proposed that opening of the M=O double bond leaves a free valence on the metal that can be used to form a second bond with the chemisorbing reactant molecule [6]. Tarama et al. [7] investigated the role of the short V=O bond in bulk V_2O_5-based and mixed V_2O_5-MoO_3 catalysts for ox-

* Corresponding author. Fax: +1 610 758 6555.
E-mail address: iew0@lehigh.edu (I.E. Wachs).

0021-9517/$ – see front matter
doi:10.1016/j.jcat.2008.03.010

idation reactions and also concluded that the strength of short V=O bond, as reflected in the IR V=O band position, is the controlling factor for catalytic oxidation, and that MoO_3 plays a promoting role.

These early publications are responsible for introducing the concept that the short M=O bond of bulk metal oxides controls the catalytic activity into the catalysis literature. The reactivity data in these studies were not normalized per unit surface area or number of exposed catalytic active sites, however. Furthermore, the short M=O bonds mentioned above are present not on the metal oxide surface where the catalytic reaction is occurring, but rather inside the bulk metal oxide lattice, which reactant molecules cannot access.

The catalysis research group of Bielanski [8] initially concluded that the short V=O bond in vanadium-based catalysts is a weak catalytic active site in nonselective oxidation reactions and does not eliminate the short V=O bond from playing a role in selective oxidation catalysis as well. Subsequently, Bielanski and Najbar went on to experimentally and theoretically demonstrate that surface V=O groups are inactive for the selective oxidation of benzene.

To quantitatively examine the hypothesis of the relationship between the short M=O bond in bulk mixed metal oxides and their catalytic reactivity, the surface reactivity of bulk metal molybdate and vanadate catalysts was investigated using CH_3OH temperature-programmed surface reaction (TPSR) spectroscopy and steady-state CH_3OH oxidation. The CH_3OH-TPSR experiment provided the first-order surface kinetic rate constants for breaking of the C–H bond of surface CH_3OH^* and CH_3O^* intermediates for the formation of HCHO and the number of catalytic active sites (N_s) [10]. The corresponding steady-state methanol CH_3OH studies provided the specific reaction rate (TOF) and the equilibrium adsorption constant (K_{ads}) that reflects breaking of the methanol O–H bond [10]. Unlike the broad IR M=O bands, Raman spectroscopy revealed sharp M=O bands that reflect the short M=O bond strength [11,12]. The present study rigorously compares, for the first time, the relationship between the normalized surface reactivity for CH_3OH oxidation to formaldehyde and the short M=O bond strengths of bulk mixed metal molybdates and vanadates.

2. Experimental

2.1. Catalyst preparation

The bulk mixed metal vanadate catalysts $AlVO_4$, $FeVO_4$, $NbVO_5$, $CrVO_4$, $Zn_3(VO_4)_2$, $Ni_3(VO_4)_2$, and $Cu_3(VO_4)_2$ were prepared through an organic route using their corresponding metal oxalates or nitrates [$Al(NO_3)_3{\cdot}9H_2O$, $Fe(NO_3)_3{\cdot}9H_2O$, $Nb(HC_2O_4)_5$, $Cr(NO_3)_3{\cdot}9H_2O$, $Zn(NO_3)_2{\cdot}6H_2O$, $Ni(NO_3)_2{\cdot}6H_2O$, and $Cu(NO_3)_2{\cdot}6H_2O$; Alpha Aesar Products, 99.9%), NH_4VO_3 (Alpha Aesar Products, 99.9%) and citric acid ($HOC(COOH)(CH_2COOH)_2{\cdot}H_2O$; Alpha Aesar Products, 99.9%] [13]. The bulk mixed metal vanadates $CeVO_4$ and $TiVO_4$ were prepared from NH_4VO_3 (Alpha Aesar Products, 99.9%), metal nitrate or oxalate ($Ce(NO_3)_4{\cdot}6H_2O$ and $HOC(COOH)(CH_2COOH)_2{\cdot}H_2O$; Alpha Aesar Products, 99.9.%), and citric acid ($HOC(COOH)(CH_2COOH)_2{\cdot}H_2O$; Alpha Aesar Products, 99.9%) [14]. The bulk metal vanadates were synthesized by dissolving a specific amount of metal nitrate/oxalate in 200 mL of distilled water to which citric acid was added, then stirred to promote complete dissolution. A stoichiometric amount of NH_4VO_3 was then added to the 200 mL of distilled water/citric acid/vanadate solution. The mixture was dried until a glassy textured solid was obtained. The precursor was further dried at room temperature overnight and then calcined at 550 °C for 6 h to form the bulk metal vanadate.

The bulk metal molybdate catalysts $Fe_2(MoO_4)_3$ and $NiMoO_4$ were synthesized by coprecipitation of their corresponding aqueous metal nitrates [$Fe(NO_3)_3{\cdot}9H_2O$ and $Ni(NO_3)_2{\cdot}6H_2O$ and $(NH_4)_6Mo_7O_{24}{\cdot}4H_2O$ (Alfa Aesar Products, 99.9%)]. First, 15 g of the metal nitrate was dissolved in 200 mL of water. The ammonium heptamolybdate was added dropwise to the metal nitrate solution under stirring. The mixture was maintained at 80 °C and a pH of 1.75 for $Fe_2(MoO_4)_3$ and a pH of 6.0 for $NiMoO_4$ by adding HNO_3. After 3 h of aging, the precipitate was filtered, washed with water, and finally dried at 100 °C overnight. The precursor was calcined at 500 °C for 4 h to synthesize these bulk metal molybdates. An organic method was used to prepare the bulk $CuMoO_4$, $Zr(MoO_4)_2$, $Cr_2(MoO_4)_3$, $ZnMoO_4$, $Ce_8Mo_{12}O_{49}$, and $Al_2(MoO_4)_3$ catalytic materials from their corresponding metal nitrates or chlorides [$Cu(NO_3)_2{\cdot}6H_2O$, $ZrCl_4$, $Cr(NO_3)_3{\cdot}9H_2O$, $Zn(NO_3)_2{\cdot}6H_2O$, $(NH_4)_2Ce(NO_3)_6$, $Al(NO_3)_3{\cdot}9H_2O$] and citric acid. A solution of ammonium heptamolybdate was added to the solution of metal nitrate and citric acid. Typically, 15 g of nitrate/chloride of molybdate metal was dissolved in 200 mL of distilled water, and 20 g of citric acid was subsequently added to the solution and stirred until completely dissolved. The mixture was dried until a glassy texture was obtained. The precursor was then dried overnight in an oven at 70 °C and calcined at 500 °C for 24 h. The $Al_2(MoO_4)_3$ and $Zr(MoO_4)_2$ precursors were calcined at 600 and 700 °C, respectively. More details on the synthesis of the bulk mixed metal molybdate catalyst are available elsewhere [15].

2.2. Raman spectroscopy

The Raman spectra were collected using a Horiba-Jobin Yvon LabRam-HR spectrometer equipped with a confocal microscope (Olympus BX-30), a 532-nm notch filter, and a single-stage monochromator (Horina-Jobin Yvon LabRam-HR) with a 900 grooves/mm grate. The Raman spectra were collected with 532-nm excitation (20 mW, YAG laser) in the 200–1000 cm^{-1} region. To minimize any laser-induced alterations of the sample, the laser power was kept below 0.5 mW. After removal of the Rayleigh scattering, the scattered laser light from the samples passed through the monochromator grating and collected with a visible sensitive LN_2-cooled CCD detector (Horiba-Jobin Yvon CCD-3000V). The spectrometer's resolution was ~1–2 cm^{-1} in the foregoing operational mode. The Raman spectra of bulk mixed metal vanadates and molybdates were collected under ambient conditions.

2.3. CH_3OH-temperature-programmed surface reaction spectroscopy

The CH_3OH-TPSR experiments were conducted on an Altamira-200 instrument coupled to a Dymaxion Dycor mass spectrometer (DME200MS) for analysis of reaction products. The experiment was computer-controlled by Dycor System 200 software. About ~0.2–0.5 g of catalyst was loaded into a glass U-tube sample holder. To remove any combustible impurities and adsorbed moisture, the samples were pretreated by calcining in air (Ultra Zero Grade, flow rate = 25 sccm) at 400 °C for 40 min. The sample was then cooled in air to 110 °C, and then flushed with He for another 30 min. Methanol was then chemisorbed on the catalyst sample by exposing it to a stream of CH_3OH/He gas with a CH_3OH concentration of 2000 ppm at 100 °C for 30 min. Previous studies have demonstrated negligible physical adsorption of CH_3OH at this adsorption temperature [16,17]. The catalyst sample was then flushed with flowing He for another 60 min at 110 °C to remove any residual CH_3OH from the system. After this, the catalyst with the chemisorbed methanol was heated to 490 °C at a rate of 10 °C/min in flowing He (30 sccm). The resulting reaction products were analyzed by the online mass spectrometer, which was switched on 30 min before the end of the flushing process to stabilize the system. The mass spectrometer m/e values used to detect the various gaseous products were as follows: CH_3OH (methanol) = 31, HCHO (formaldehyde) = 30, CH_3OCH_3 (dimethyl ether/DME) = 45, CH_3OOCH (methyl formate/MF) = 60, $(CH_3O)_2CH_2$ (dimethoxy methane/DMM) = 75, H_2O (water) = 18, CO (carbon monoxide) = 28, CO_2 (carbon dioxide) = 44. Only negligible amounts of CO and CO_2 products were detected in the bulk vanadate and molybdate catalysts.

HCHO was the major reaction product formed during CH_3OH-TPSR over the bulk mixed metal vanadate and molybdate catalysts. The negligible amounts of CO/CO_2 produced during CH_3OH-TPSR reflect the small contribution of HCHO readsoprtion to the TPSR spectra, because readsorption is known to lead to overoxidation of HCHO to CO/CO_2 [17]. Thus, the HCHO/CH_3OH-TPSR spectra contain kinetic information on HCHO molecules that did not readsorb in the catalyst bed. The HCHO T_p values were determined by fitting a Gaussian curve through the raw mass spectroscopy data using commercial software that can determine the T_p value within an accuracy of ±1 °C.

The Redhead equation [18] was applied to calculate the activation energy, E_a, for the first-order rate constant involved in breaking the C–H bond of chemisorbed methanol; this is expressed as

$$\frac{E_a}{RT_p^2} = \frac{\upsilon}{\beta}\exp\left(-\frac{E_a}{RT_p}\right), \tag{1}$$

where E_a is the activation energy for the reaction (kcal/mol), R is the universal gas constant (kcal/kg mol-K), T_p is the temperature of the desorption peak maximum (K), υ is the pre-exponential factor (s^{-1}), and β is the constant heating rate (10 °C/min).

Previous investigations have shown that the formation of HCHO from CH_3OH follows first-order reaction kinetics [19]. Recent DFT calculations by Sauer's group have predicted that the first-order pre-exponential factor for the decomposition of surface methoxy (CH_3O^*) to formaldehyde over vanadia-based catalysts should be $\sim 0.3 \times 10^{13}$ s^{-1} [20]. Consequently, the ideal first-order pre-exponential value of $\upsilon = 10^{13}$ s^{-1} was used in the present study to calculate the E_a values from Eq. (1) [18].

The first-order rate constant for the rate-determining step, k_{rds}, is represented by the expression

$$k_{rds}\left(s^{-1}\right) = \upsilon\exp\left(-\frac{E_a}{RT_{ref}}\right), \tag{2}$$

in which T_{ref} represents the reference reaction temperature. For k_{rds} and K_{ads} calculations, T_{ref} of 300 and 380 °C are used for bulk vanadates and molybdates samples, respectively.

Care should always be taken while conducting temperature-programmed analysis to avoid limitations such as diffusion limitations, readsorption, and time-lag during the execution of the experiment, because these effects can perturb the observed T_p values as well as the shape of the desorption curves [21]. In such situations, the E_a value calculated from Eq. (2) will deviate from the true surface reaction activation energy. This problem becomes significant when the desorbing molecule readsorbs multiple times in the catalyst bed before reaching the detector (e.g., CO/CO-TPD from supported precious metal catalysts) [21]. For TPSR experiments involving surface reactions, however, the reaction products will usually undergo further reaction when significant readsorption occurs in the catalyst bed before reaching the mass spectroscopy (e.g., readsorption of HCHO leads to CO/CO_2 formation). Thus, during TPSR experiments, the readsorbing HCHO is converted to CO/CO_2, and only the surviving HCHO reaction product from methanol oxidation is minimally affected by readsorption and carries the fundamental surface kinetic information to the mass spectroscopy. This is why essentially the same T_p and FWHM (full width at half maximum) values are obtained for HCHO/CH_3OH-TPSR from metal oxide powders in vacuum and at atmospheric pressure [22].

2.4. Steady-state methanol oxidation

Steady-state methanol oxidation was carried out in a fixed-bed catalytic reactor under differential reaction conditions (methanol conversion ⩽10%). During this process, care was taken to avoid heat and mass transfer limitations [23]. The oxidation reactions were performed with a feed gas composition of 6/13/81 mol% (methanol/oxygen/helium) and a total flow rate of 100 cm^3 (NTP) min^{-1}. Methanol oxidation over the bulk mixed vanadates and molybdates were performed at 300 and 380 °C, respectively. The reaction products were analyzed and quantified with an online gas chromatograph (HP 5840) equipped with thermal conductivity and flame ionization detectors and two columns: a capillary column (CP-sil 5CB) for dimethyl methane, dimethyl ether, methyl formate, and CH_3OH analysis, and a packed column (Carboxene-1000) for CO, CO_2, O_2, HCHO, and CH_3OH analysis.

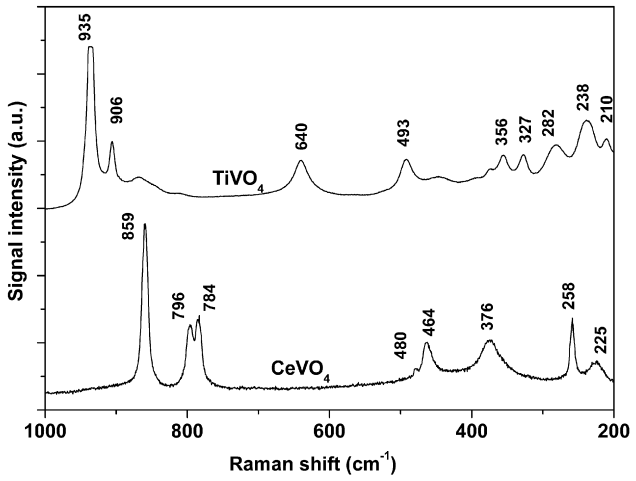

Fig. 1. Raman spectra of bulk $CeVO_4$, and $TiVO_4$.

The steady-state turnover frequency (TOF; molecules of HCHO formed per exposed catalytic active site per second) values for the bulk mixed metal vanadate and molybdate catalysts have been reported previously [13,15]. The number of exposed catalytic active sites was determined by CH_3OH chemisorption.

The CH_3OH adsorption equilibrium constant, K_{ads} (atm^{-1}), also could be determined by combining the k_{rds} values from CH_3OH-TPSR and the corresponding TOF values from the steady-state reaction kinetics,

$$\text{TOF}\ (s^{-1}) = k_{rds} K_{ads} P_{CH_3OH}, \tag{3}$$

where K_{ads} is the CH_3OH adsorption equilibrium constant and P_{CH_3OH} is the partial pressure of CH_3OH (atm).

Rearranging, we have

$$K_{ads}\ (atm^{-1}) = \text{TOF}/(k_{rds} P_{CH_3OH}). \tag{4}$$

The first-order kinetics with respect to CH_3OH partial pressure and zero-order kinetics with respect to molecular O_2 partial pressure over bulk metal molybdates and vanadates are well established [10]. The reaction is zero-order with respect to gas-phase molecular O_2, because the catalyst is fully oxidized under reaction conditions, and the reaction uses bulk lattice oxygen from the mixed metal oxide catalysts (i.e., the Mars–van Krevelen reaction mechanism [4]).

3. Results

3.1. Raman spectroscopy

The phase purity of the bulk mixed vanadates and molybdates was determined by Raman spectroscopy because of this technique's high sensitivity toward crystalline V_2O_5 and MoO_3 nanoparticles. Representative Raman spectra of the bulk $CeVO_4$ and $TiVO_4$ mixed oxides are presented in Fig. 1. These spectra agree well with those reported in the literature and do not exhibit the Raman vibrations of crystalline V_2O_5 (994, 689, 403, and 278 cm^{-1}) [24,25]. The Raman spectra for bulk mixed metal vanadates of $AlVO_4$, $Cu_3(VO_4)_2$, $CrVO_4$, $FeVO_4$, $Ni_3(VO_4)_2$, $NbVO_5$, and $Zn_3(VO_4)_2$ have been reported previously [13]. The Raman spectra of the bulk mixed metal molybdates of $Cr_2(MoO_4)_3$, $Fe_2(MoO_4)_3$, $Zr(MoO_4)_2$, $ZnMoO_4$, $NiMoO_4$, $Al_2(MoO_4)_3$, $CuMoO_4$, and $Ce_8Mo_{12}O_{49}$ also have been reported previously and shown to be phase-pure and free of crystalline MoO_3 nanoparticles (999, 819, 668, and 291 cm^{-1}) [15].

Table 1
Kinetic parameters for bulk mixed metal vanadate catalysts

Compounds	T_p (°C)	k_{rds}[a] (s^{-1})	K_{ads}[a] (atm^{-1})	TOF[a,b] (s^{-1})
$AlVO_4$	198	5.5	7	2.2
$CeVO_4$	193	7.5	–	N.D.
$CrVO_4$	186	12	21	14
$Cu_3(VO_4)_2$	203	4.0	26	6.2
$FeVO_4$	201	4.6	10	4.0
$NbVO_5$	191	8.5	6	3.1
$Ni_3(VO_4)_2$	213	2.2	33	4.3
$TiVO_4$	188	10	–	N.D.
$Zn_3(VO_4)_2$	230	0.76	4	0.2
V_2O_5	200	4.9	5	1.5

[a] Obtained at $T = 300$ °C.
[b] Obtained from [13].

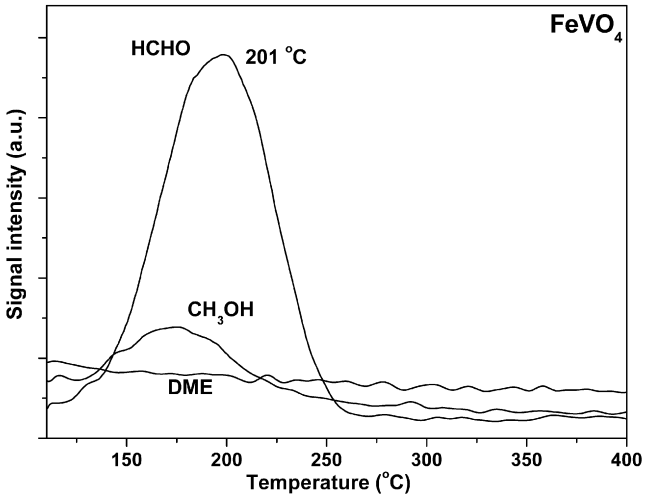

Fig. 2. CH_3OH-TPSR spectrum from bulk $FeVO_4$.

3.2. CH_3OH-TPSR spectroscopy

The CH_3OH-TPSR spectra from the bulk mixed metal vanadates of $AlVO_4$, $FeVO_4$, $NbVO_5$, $CrVO_4$, $Zn_3(VO_4)_2$, $Ni_3(VO_4)_2$, $Cu_3(VO_4)_2$, $CeVO_4$, and $TiVO_4$ catalysts yielded predominantly HCHO as the reaction product; the corresponding T_p values are given in Table 1. The selective formation of HCHO reflects the redox nature of the bulk mixed vanadate catalytic materials; for example, in the CH_3OH-TPSR spectra from bulk $FeVO_4$, presented in Fig. 2, HCHO is the sole reaction product, with a T_p of 201 °C. In the HCHO/CH_3OH-TPSR spectra from the bulk vanadium oxide catalysts, shown in Fig. 3, the HCHO T_p values vary over a wide temperature range for the catalysts, reflecting the different intrinsic activities of the vanadate catalysts. The kinetic k_{rds}, K_{ads}, and TOF parameters for methanol oxidation to formaldehyde over the bulk mixed metal vanadate catalysts at 300 °C are also given in Table 1.

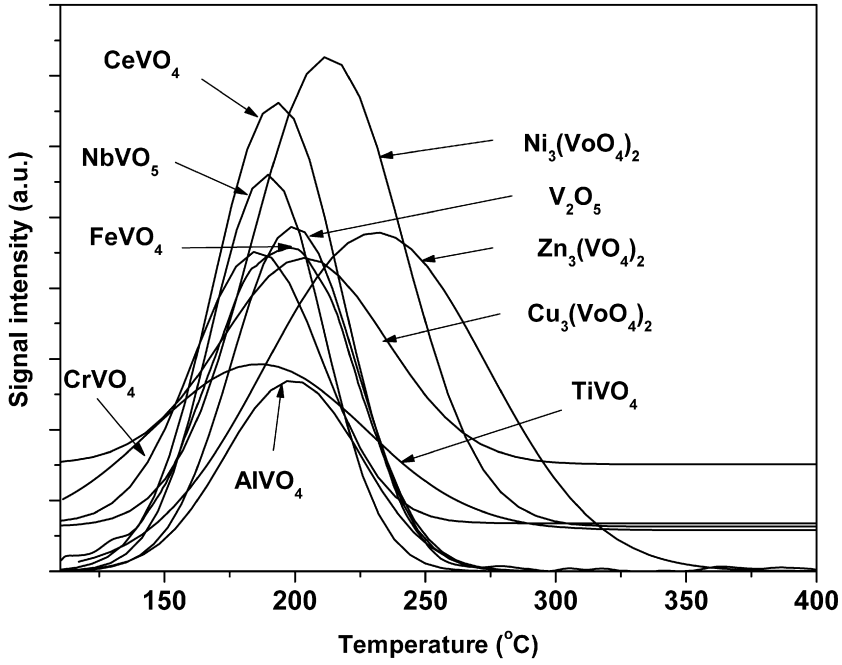

Fig. 3. CH_3OH-TPSR spectra from bulk $AlVO_4$, $CeVO_4$, $CrVO_4$, $Cu_3(VoO_4)_2$, $FeVO_4$, $NbVO_5$, $Ni_3(VO_4)_2$, $TiVO_4$, $Zn_3(VO_4)_2$, and V_2O_5.

Table 2
Kinetic parameters for bulk mixed metal molybdate

Compounds	T_p (°C)	k_{rds}[a] (s^{-1})	K_{ads}[a] (atm^{-1})	TOF[a,b] (s^{-1})
$Al_2(MoO_4)_3$	225	0.67	44	1.8
$Ce_8Mo_{12}O_{49}$	201	2.5	22	3.3
$Cr_2(MoO_4)_3$	201	2.5	23	3.4
$CuMoO_4$	220	0.88	19	1.0
$Fe_2(MoO_4)_3$	209	1.2	24	2.3
$NiMoO_4$	250	0.17	86	0.9
$ZnMoO_4$	237	0.35	57	1.2
$Zr(MoO_4)_2$	215	1.2	518	36
MoO_3	205	2	37	4.5

[a] Obtained at $T = 380\,°C$.
[b] Obtained from [15].

The CH_3OH-TPSR spectra from the bulk metal molybdate catalysts yielded predominantly HCHO as the reaction product; their T_p values are given in Table 2. The selective formation of HCHO reflects the redox nature of the bulk mixed metal molybdate catalytic materials. For example, in the CH_3OH-TPSR spectra from bulk $Fe_2(MoO_4)_3$, shown in Fig. 4, HCHO is the sole reaction product, with a T_p of 209 °C. In the HCHO/CH_3OH-TPSR spectra from the bulk molybdenum oxide catalysts, presented in Fig. 5, the HCHO T_p values vary over a wide temperature range, reflecting the different intrinsic activities of the molybdate catalysts. The kinetic k_{rds}, K_{ads}, and TOF parameters for methanol oxidation over the bulk mixed metal molybdate catalysts at a reaction temperature of 380 °C are given in Table 2.

4. Discussion

The aim of the present study was to investigate whether the strength or length of the short M=O bond correlates with the catalytic activity of the bulk mixed metal vanadates and molybdate catalysts for methanol oxidation to formaldehyde.

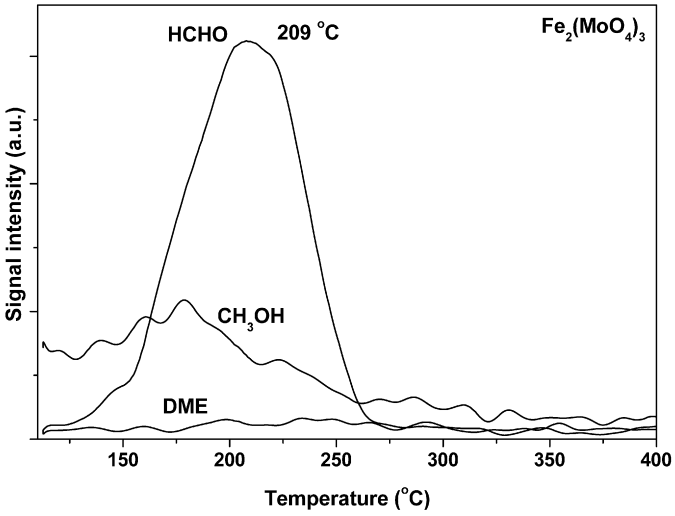

Fig. 4. CH_3OH-TPSR spectrum from bulk $Fe_2(MoO_4)_3$.

4.1. Relationship between the short M=O bond length and the surface catalytic activity of bulk mixed metal oxides (crystallographic M=O bond lengths)

The bond lengths of short M=O bonds in the bulk mixed metal vanadates and molybdates, obtained from crystallographic literature studies, are given in Tables 3 and 4, respectively. The CH_3OH-TPSR surface kinetic parameters for the rate-determining step, k_{rds}, in HCHO formation over the bulk mixed metal vanadates and molybdates are plotted against the crystallographic short M=O bond length in Fig. 6. No par-

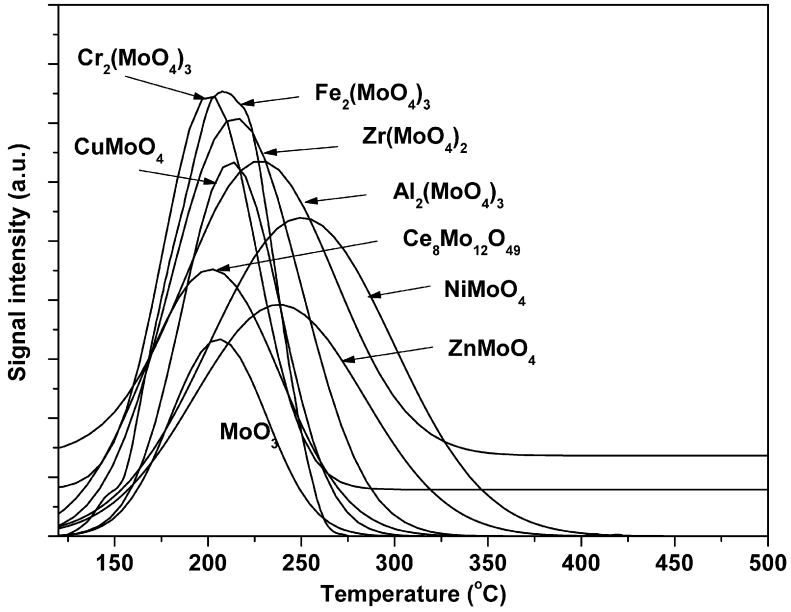

Fig. 5. CH_3OH-TPSR spectra from bulk $Al_2(MoO_4)_3$, $Ce_8Mo_{12}O_{49}$, $Cr_2(MoO_4)_3$, $CuMoO_4$, $Fe_2(MoO_4)_3$, $NiMoO_4$, $ZnMoO_4$, $Zr(MoO_4)_2$, and MoO_3.

Table 3
Raman vibrations of V=O in bulk mixed vanadates and their corresponding bond lengths from crystallographic studies

Compounds	V=O bond length (A°) [reference]	Raman vibration of V=O (cm^{-1})
$AlVO_4$	1.59 [12]	966
$CeVO_4$	1.7 [26]	859
$CrVO_4$	1.72 [27]	924
$Cu_3(VO_4)_2$	1.67 [28]	867
$FeVO_4$	1.65 [29]	934
$NbVO_5$	N.D.	1003
$Ni_3(VO_4)_2$	1.7 [30]	960
$TiVO_4$	N.D.	947
$Zn_3(VO_4)_2$	1.67 [31]	861
V_2O_5	1.58 [12]	994

Table 4
Raman vibrations of Mo=O in bulk mixed molybdates and their corresponding bonds length from crystallographic studies

Compound	Mo=O bond length (A°) [reference]	Raman vibration of Mo=O (cm^{-1})
$Al_2(MoO_4)_3$	1.70 [32]	1008
$Ce_8Mo_{12}O_{49}$	N.D.	950
$Cr_2(MoO_4)_3$	1.6 [33]	962
$CuMoO_4$	1.70 [11]	968
$Fe_2(MoO_4)_3$	1.58 [34]	964
$NiMoO_4$	N.D.	961
$ZnMoO_4$	1.71 [34]	951
$Zr(MoO_4)_2$	N.D.	974
MoO_3	1.67 [12]	998

ticular correlation can be seen between the short M=O bond lengths in the bulk mixed vanadates and molybdates and the surface catalytic activity, indicating that the length of the short M=O bond is not a controlling factor in oxidation reactions over bulk mixed metal oxides.

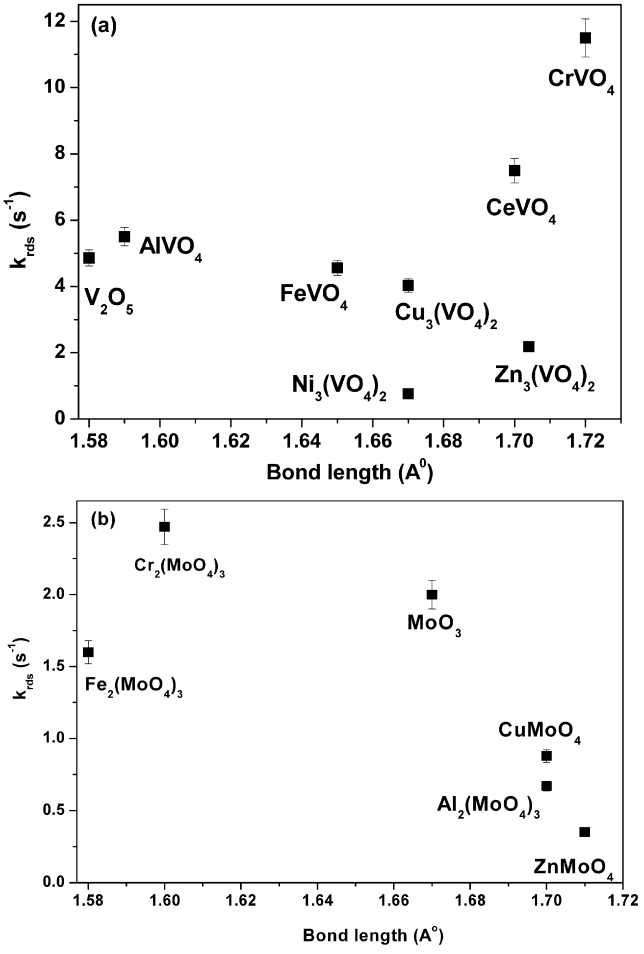

Fig. 6. Plots of first-order rate constant (k_{rds}) for surface methoxy decomposition vs the crystallographic short M=O bond length for (a) bulk mixed metal vanadates and (b) bulk mixed metal molybdates. The bars show the ±5% error associated with the k_{rds} values.

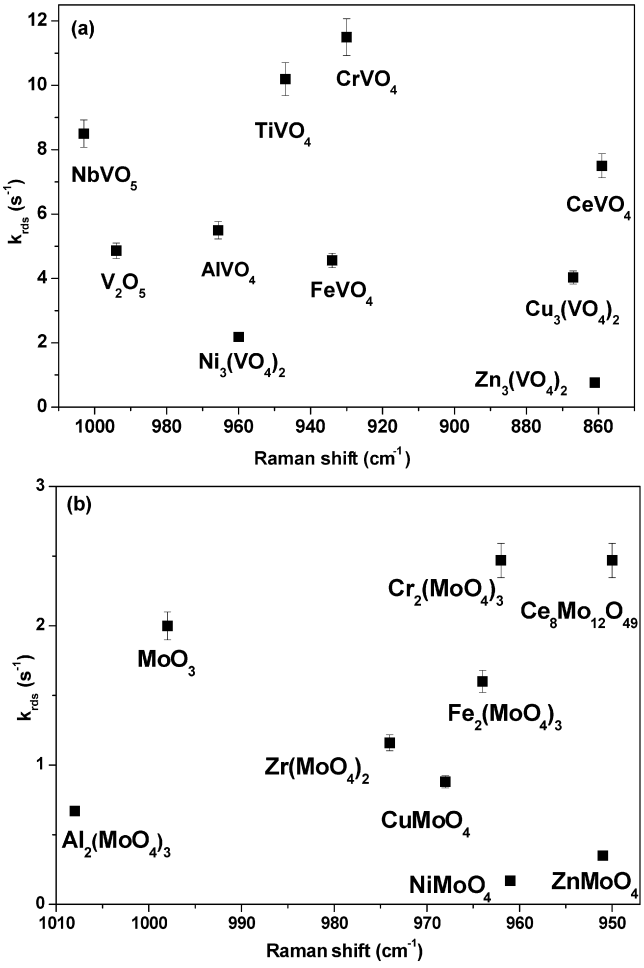

Fig. 7. Plots of first-order rate constant (k_{rds}) for surface methoxy decomposition vs the Raman shift of short M=O for (a) bulk mixed metal vanadates and (b) bulk mixed metal molybdates. The bars show the ±5% error associated with the k_{rds} values.

4.2. Relationship between the short M=O bond length and the surface catalytic activity of bulk mixed metal oxides (M=O bond length from Raman spectra)

Earlier studies compared the catalytic activity with the M=O IR vibrations of bulk mixed metal oxides [5–9]. As mentioned earlier, the IR bands for the bulk M=O bonds generally give rise to broad bands that are much better resolved with Raman spectroscopy because of the sharper Raman bands. The short M=O Raman band positions of bulk mixed metal vanadates and molybdates are listed in Tables 3 and 4; longer M=O bonds generally give rise to lower wavenumber values. The correlations between the short M=O Raman band positions and the methanol oxidation to HCHO rate-determining step k_{rds} are shown in Fig. 7. The figure shows no apparent relationship between the length of the short M=O bond and the surface catalytic activity. Again, there appears to be no relationship between the length of the short M=O bond obtained from vibrational spectroscopy and the surface catalytic activity of bulk mixed metal vanadates and molybdates.

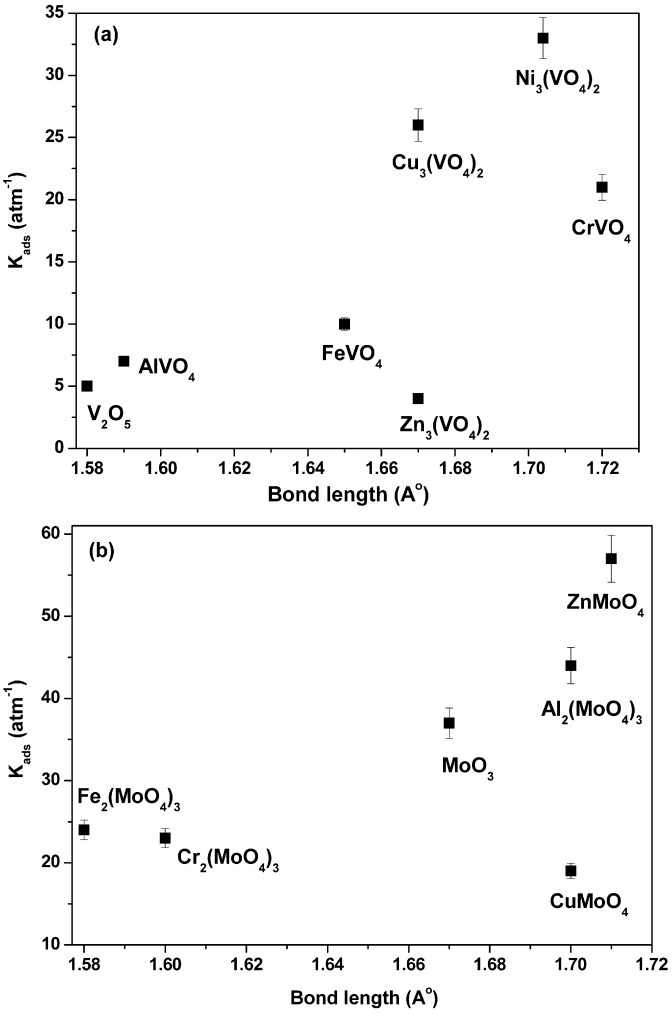

Fig. 8. Plots of CH_3OH equilibrium adsorption constant (K_{ads}) vs the crystallographic short M=O bond length for (a) bulk mixed metal vanadates and (b) bulk mixed metal molybdates. The bars show the ±5% error associated with the K_{ads} values.

4.3. Relationship between the short M=O bond length and the K_{ads} (CH_3OH adsorption equilibrium constant) of bulk mixed metal oxides (crystallographic M=O bond lengths)

Figs. 8 and 9 show the methanol adsorption equilibrium constants (K_{ads}), which reflect the ease of breaking the methanol O–H bond on adsorption, for bulk mixed metal vanadates and molybdates. K_{ads} is plotted against the short M=O bond length obtained from crystallographic studies in Fig. 8 and against the M=O Raman shift in Fig. 9. The plots demonstrate no particular relationship between the short M=O bond length and the methanol equilibrium adsorption constant.

4.4. Relationship between the short M=O bond length and the steady-state catalytic TOF of bulk mixed metal vanadates and molybdates

Fig. 10 plots the steady-state TOF values for CH_3OH oxidation over the bulk mixed vanadate and molybdate catalysts as a function of the M=O Raman shift. Fig. 11 presents cor-

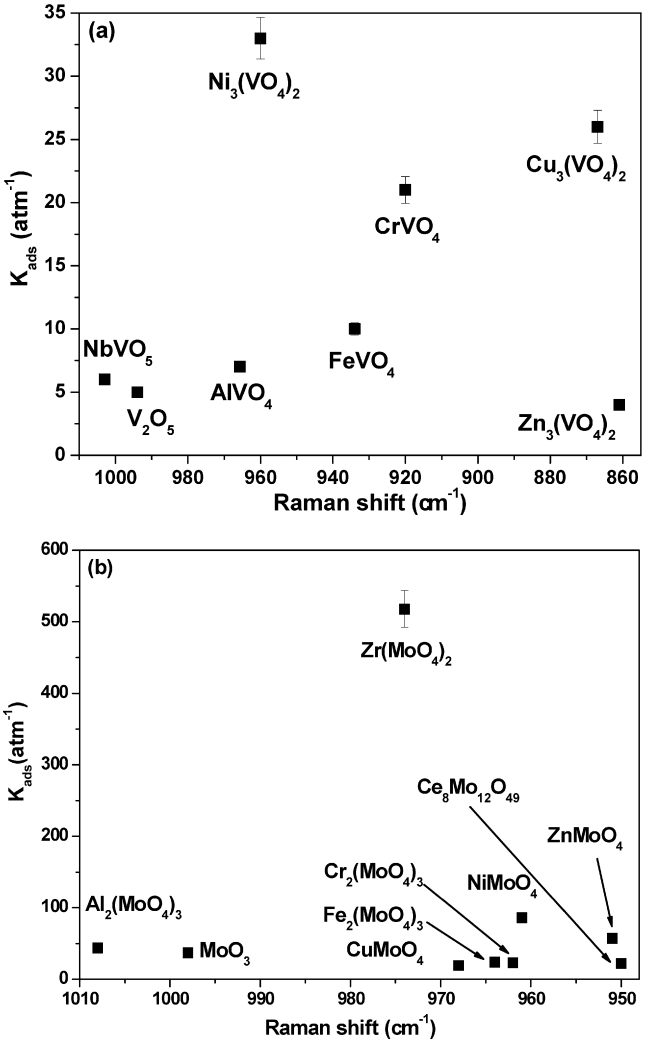

Fig. 9. Plots of CH_3OH equilibrium adsorption constant (K_{ads}) vs the Raman shift of short M=O bond for (a) bulk mixed metal vanadates and (b) bulk mixed metal molybdates. The bars show the ±5% error associated with the K_{ads} values.

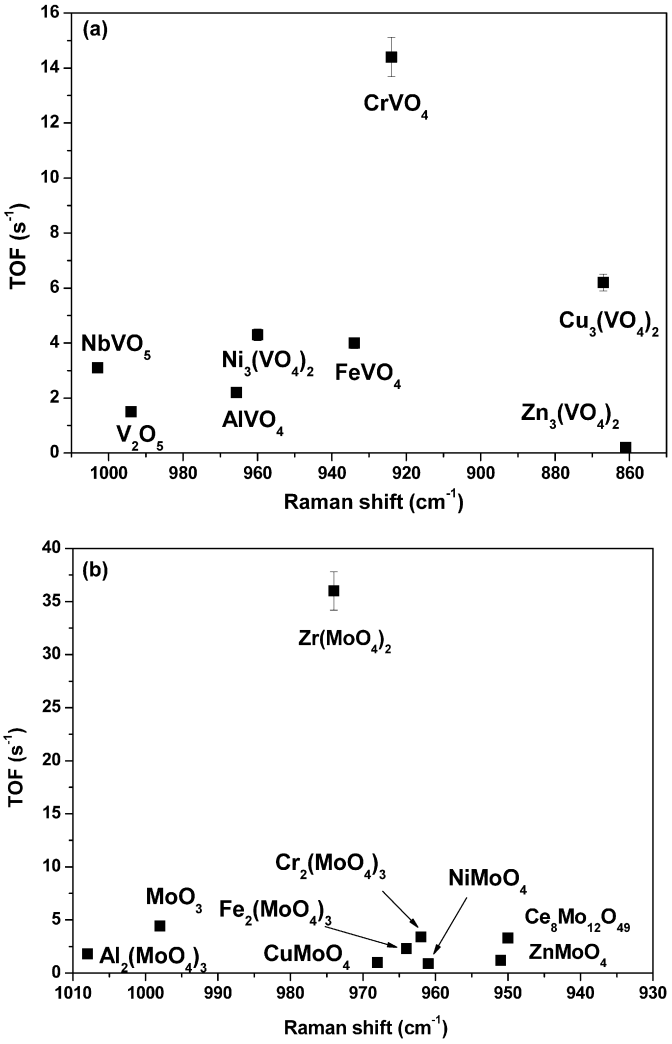

Fig. 10. Plots of the steady-state TOF for CH_3OH oxidation to HCHO vs the Raman shift of short M=O bond for (a) bulk mixed metal vanadates and (b) bulk mixed metal molybdates. The bars show the ±5% error associated with the TOF values.

responding plots of methanol oxidation TOF versus the short M=O bond length determined crystallographically. Recall that the number of exposed catalytic active sites was determined by methanol chemisorption, which is the most appropriate chemical probe molecule because it also is the reactant for this reaction. Most of the TOF values for steady-state CH_3OH oxidation to HCHO are scattered around the same value, with one or two outlying data points. Again, no correlations can be seen between the TOF for methanol oxidation to formaldehyde and the short M=O bond length (strength) of the bulk mixed metal vanadates and molybdates.

5. Conclusion

Our findings demonstrate no rigorous support for a relationship between the bulk M=O bond strength or length and the specific reaction rate k_{rds}, adsorption equilibrium constant K_{ads}, and steady-state TOF for CH_3OH oxidative dehydrogenation to HCHO over bulk mixed metal vanadate and molybdate catalysts. The absence of a relationship between the short M=O bond length and the intrinsic catalytic activity for CH_3OH oxidative dehydrogenation is not surprising for several reasons. First, the rate-determining step in the CH_3OH oxidative dehydrogenation reaction is the C–H bond breaking step [5], which does not involve bulk M=O bond breaking. Second, the CH_3OH adsorption step is the O–H bond breaking step and does not involve bulk M=O bond breaking. Thus, the properties of the short M=O bond strength or length should not affect the specific oxidative dehydrogenation reaction rate (TOF). Third, the short M=O bond lengths used in these correlations are the bulk crystalline values, not those of the catalytic active sites present on the outermost surface of bulk mixed metal vanadate and molybdate catalytic materials. The surface compositions and structures of the bulk mixed metal oxides differ greatly from the bulk structures, and the surfaces tend to be enriched with surface VO_x and MoO_x overlayers [12,14]. Consequently, attempting to correlate surface catalytic kinetic data with bulk metal oxide M=O structures is not scientifically rigorous and is

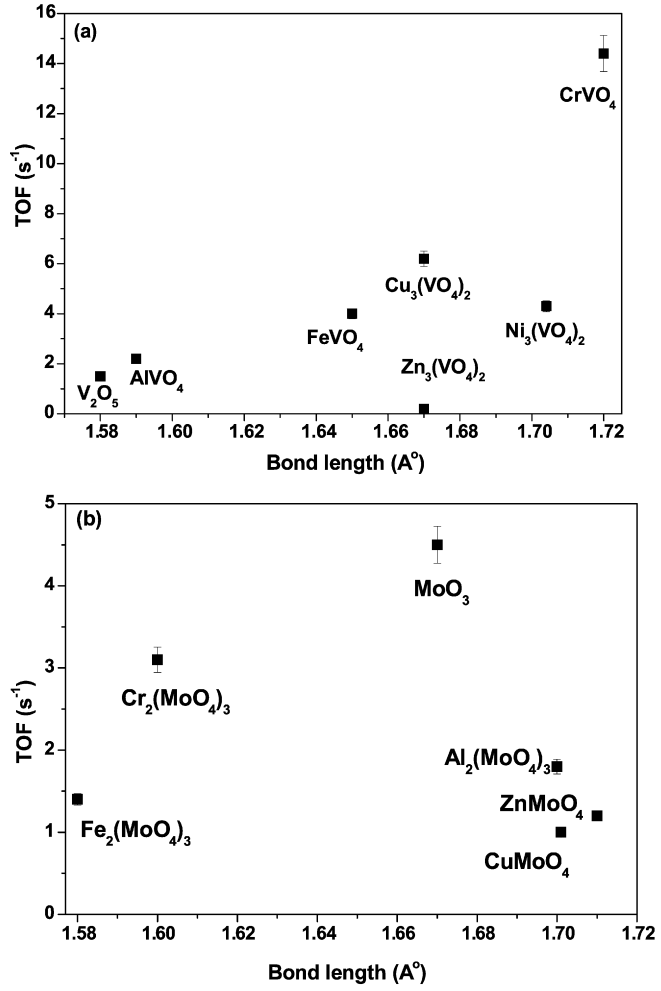

Fig. 11. Plots of steady-state TOF for CH_3OH oxidation to HCHO vs the crystallographic short M=O bond length for (a) bulk mixed metal vanadates and (b) bulk mixed metal molybdates. The bars show the ±5% error associated with the TOF values.

quite inappropriate. Clearly, more detailed information on surface composition and structure is needed to fully understand the nature of the catalytic active sites present on the surface of bulk mixed metal oxides and their relationship to catalytic activity.

Acknowledgments

Financial support was provided by the US Department of Energy (Basic Energy Sciences Grant DE-FG02-93ER14350) and the International NSF (USA)-CONICET (Argentina) program (research No. 0060). The authors thank Taejin Kim for assisting with the CH_3OH-TPSR experiments.

References

[1] H. Adkins, W.R. Pederson, J. Am. Chem. Soc. 53 (1931) 1512.
[2] R.K. Grasselli, J.D. Burrington, Adv. Catal. 30 (1981) 133.
[3] H. Imai, Y. Kamiya, T. Okuhara, J. Catal. 251 (2007) 195.
[4] P. Mars, D.W. van Krevelen, Chem. Eng. Sci. 3 (1954) 41.
[5] F. Trifiro, P. Centola, I. Pasquon, J. Catal. 10 (1968) 86.
[6] F. Trifiro, I. Pasquon, J. Catal. 12 (1968) 412.
[7] K. Tarama, S. Teranishi, S. Yoshida, N. Tamura, in: Proc. of 3rd Int. Congr. Catalysis, Amsterdam, 1965, 282.
[8] A. Bielanski, A. Inglot, React. Kinet. Catal. Lett. 6 (1977) 83.
[9] A. Bielanski, M. Najbar, Appl. Catal. A 157 (1997) 223.
[10] W.L. Holstein, C.J. Machiels, J. Catal. 162 (1996) 118.
[11] F.D. Hardcastle, I.E. Wachs, J. Raman Spectrosc. 21 (1990) 683.
[12] F.D. Hardcastle, I.E. Wachs, J. Phys. Chem. 95 (1991) 5031.
[13] L.E. Briand, J.-M. Jehng, L. Cornaglia, A.M. Hirt, I.E. Wachs, Catal. Today 78 (2003) 257.
[14] C.T. Au, W.D. Zhang, H.L. Wan, Catal. Lett. 37 (1996) 241.
[15] L.E. Briand, A.M. Hirt, I.E. Wachs, J. Catal. 202 (2001) 268.
[16] J.M. Tatibouët, Appl. Catal. A 148 (1997) 213.
[17] L.E. Briand, W.E. Farneth, I.E. Wachs, Catal. Today 62 (2000) 219.
[18] J.W. Niemantsverdriet, Spectroscopy in Catalysis, second ed., Wiley–VCH, Weinheim, 2000.
[19] W.L. Holstein, C.J. Machiels, J. Catal. 162 (1996) 118.
[20] J. Döbler, M. Pritzsche, J. Sauer, J. Am. Chem. Soc. 127 (2005) 10862.
[21] R.J. Gorte, J. Catal. 75 (1982) 164.
[22] W.E. Farneth, F. Ohuchi, R.H. Staley, U. Chowdhry, A.W. Sleight, J. Phys. Chem. 89 (1985) 2439.
[23] K. Routray, G. Deo, AIChE J. 51 (2005) 1733.
[24] U.O. Krasovec, B. Orel, A. Surca, N. Bukovec, R. Reisfeld, Solid State Ionics 118 (1999) 195.
[25] C.L. Lieck, M.A. Banares, M.A. Vicente, J.L.G. Fierro, Chem. Mater. 13 (2001) 1174.
[26] B.C. Chakoumakos, M.M. Abraham, L.A. Boatner, J. Solid State Chem. 109 (1994) 197.
[27] R.J. Riedner, L. Cartz, J. Appl. Phys. 42 (1971) 5177.
[28] R.D. Shannon, C. Calvo, Can. J. Chem. 50 (1972) 3944.
[29] B. Robertson, E. Kostiner, J. Solid State Chem. 4 (1972) 29.
[30] E.E. Sauerbrei, R. Faggiani, C. Calvo, Acta Crystallogr. 29 (1973) 2304.
[31] R. Gopal, C. Calvo, Can. J. Chem. 49 (1971) 3056.
[32] W.T.A. Harrison, A.K. Cheetham, J. Faber Jr., J. Solid State Chem. 76 (1988) 328.
[33] P.D. Battle, A.K. Cheetham, W.T.A. Harrison, N.J. Pollard, J. Solid State Chem. 58 (1985) 221.
[34] J.C.J. Bart, N. Burriesci, M. Petrera, Z. Phys. Chem. 132 (1982) 201.